Head wave identification in an offset vertical seismic profile

Paul Fowler

Abstract

In vertical seismic profiling (VSP), if the shot location is offset sufficiently far from the well hole, converted and post-critical (head) waves may be generated and be identified on the profile. An interface with high velocity contrast must be present at a depth which is not too much greater than the offset if a head wave is to be observed in the data. For a wide range of interface dips, if a head wave can exist, it will always arrive earlier than the direct wave for the geophone at the head wave interface. Because the head wave is an upgoing event, the curve delineated by the first arrivals on a depth-time profile can show reversals in slope creating a local maximum followed by a local minimum. Simple geometric modeling of travel times can provide criteria for the presence or absence of head waves in offset VSP data and aid in their recognition.

Introduction

In most VSP experiments, the offset of the shot from the well is small compared to the depth of the geophones or of the geologic features of interest. In this paper some effects arising from using a shot offset comparable in magnitude to the geophone depths are considered. Several motivations exist for offsetting the shot. Hardage (1981) and Balch et al. (1982) point out the importance of offset in minimizing undesired tube waves. Ullman (1982) suggests using variable offsets for discriminating between diffractions and direct arrivals. Wyatt and Wyatt (1981) use the greater lateral extent of the useful information contained in offset profiles to produce a subsurface image extending away from the well in a process they call 'VSP CDP stacking'.

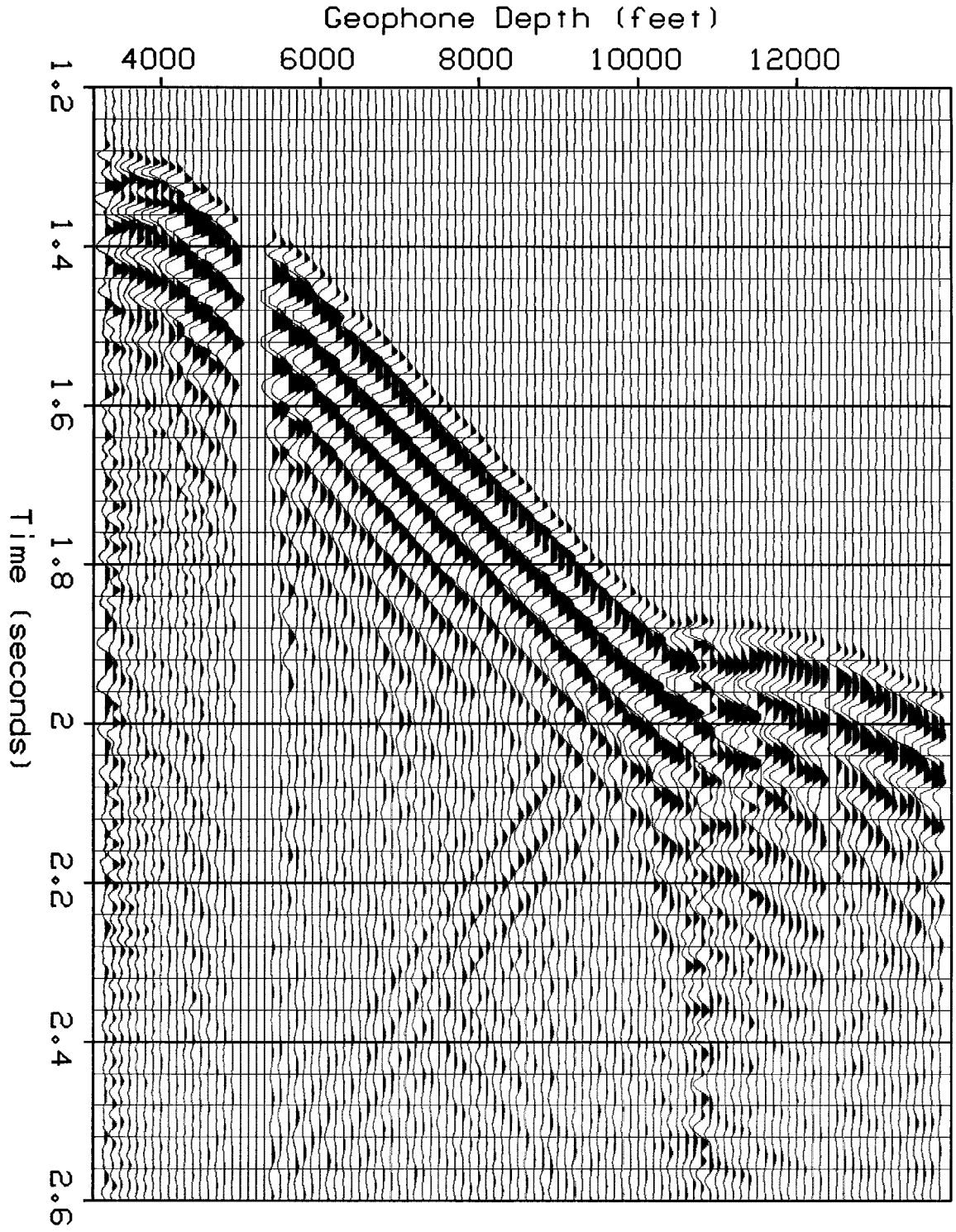

FIG. 1. Example of offset VSP data (courtesy of Amoco and Western Geophysical). The shot in this example was offset 7000 feet from the well.

Incorporating substantial offsets in VSP necessitates consideration of events which would not be seen if all waves were travelling nearly vertically, as they are in VSP with small offsets. Lash (1980,1982) discusses compressional to shear converted waves in VSP; these should be more readily observable with large offset. Another possible arrival would be a refracted or head wave. To my knowledge, this possibility has been considered principally by Russian authors; Gal'perin (1974) also derives many of the equations I use here, along with a wide variety of other related results. In this paper I examine a recorded example (of higher quality than those shown in Gal'perin's book) of offset VSP in which a head wave and a P-S conversion are visible.

An example of offset VSP data

Figure 1 displays a portion of an offset VSP record provided by Amoco and Western Geophysical Company. Geophone depths in the well hole range from 3300 feet to 13800 feet. The shot was offset 7000 feet from the well. These data posses several distinctive features. The direct arrivals show more curvature at shallow depths than on most VSP records; this is an immediate consequence of offsetting the shot. A prominent reflector causing upgoing reflections occurs at a depth of 10700 feet. Two features of the data near the depth of this reflector stand out. First, the slope of the direct arrival curve changes sharply. Close examination reveals that it actually reverses and forms a 'hump', implying that the first arrival near the interface is actually an upgoing wave, rather than the downgoing direct arrival. Also, an event may be seen continuing below the reflector with slope similar to that of the direct arrival above, as if the upper event continued on through the interface with nearly unchanged velocity. I attribute this event to a shear wave generated from the downgoing compressional wave by conversion at the interface. This event is partially obscured by the long first break waveform. I tried predictive deconvolution to shorten the first break waveform but did not succeed in making the converted event significantly more distinct.

The geometry of ray paths in offset VSP

For the study of traveltimes, a simple earth model will be used comprising a single constant velocity layer over a half-space of constant, higher velocity. This is shown in Figure 2a, along with the appropriate geometry of a VSP experiment.

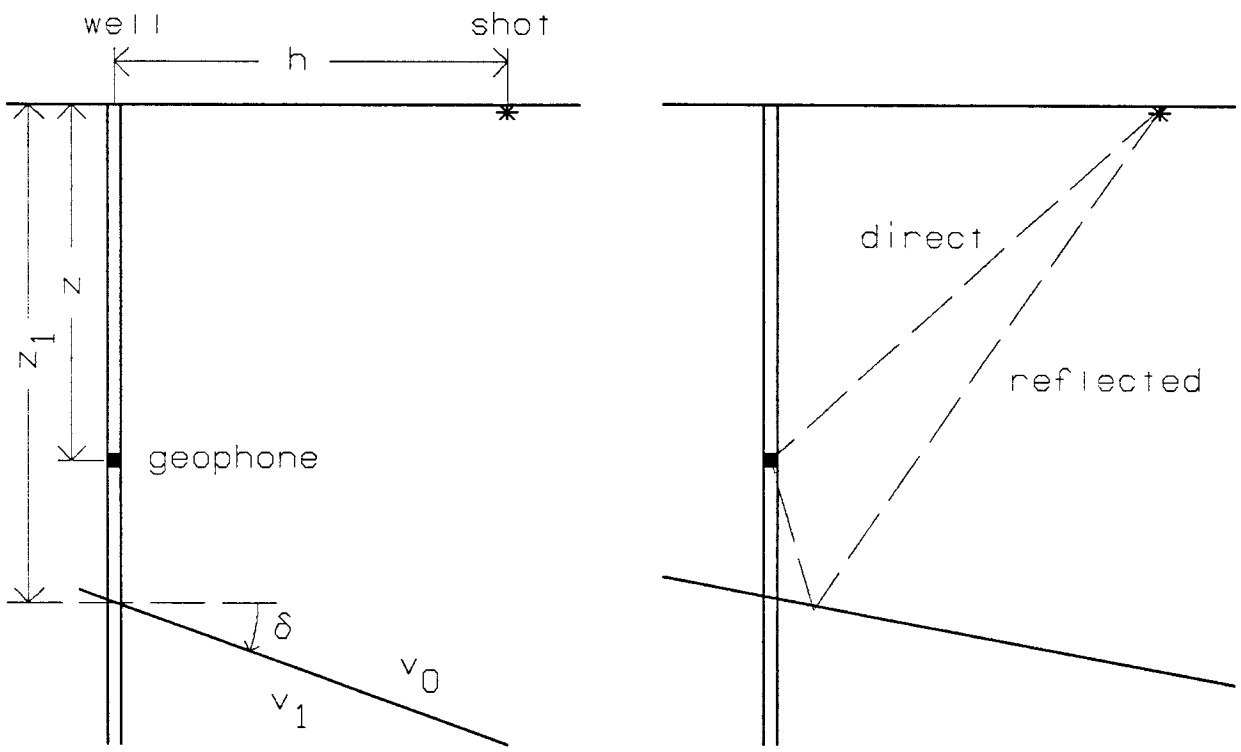

FIG. 2. (a) Geometry of an offset VSP (b) Ray paths for direct and reflected arrivals

The symbols used in Figure 2 and elsewhere in this paper are:

h	horizontal offset of the shot from the well
z	depth of a given geophone in the well
z_1	depth to the interface
δ	dip angle of the interface, measured downward from horizontal
v_0	seismic velocity in the upper medium
v_1	seismic velocity in the lower medium
θ_c	critical angle for a ray incident from above

Note that the dip angle δ is being measured downward from horizontal on the side of the well toward the shot. The relations derived below will hold for interfaces dipping upward toward the shot as well if the dip angle δ is understood to be negative. Some limitations on δ are needed. The interface must not surface between the shot and well, so the relation $\delta > -\tan^{-1}(h/z_1)$ must hold. Only reflected rays with reflection points between the shot and well are considered here, so beds dipping downward toward the shot must have

$\delta < (1/2)\tan^{-1}(h/z_1)$. This restriction also prevents consideration of reflected rays traveling vertically directly up the well hole. A similar restriction to avoid vertical rays from the head wave requires that $\delta < \theta_c = \sin^{-1}(v_0/v_1)$. These restrictions on the dip will be assumed to hold henceforth.

The ray paths for the direct and reflected arrivals are shown in Figure 2b. For a geophone at depth z less than z_1, traveltime for a direct arrival from the shot is seen immediately from Pythagoras' Theorem to be

$$t_d = \frac{1}{v_0}(h^2+z^2)^{1/2}. \tag{1}$$

The traveltime for the reflected arrival then can be shown to be

$$t_r = \frac{1}{v_0}\left[h^2+\left[(2z_1-z)\cos\delta+h\sin\delta\right]^2\right]^{1/2} \tag{2}$$

The ray path for a head wave is shown in Figure 3a. No head wave can be possible for an interface dipping too steeply downwards towards the shot. Specifically, the limit is given by $\cos\delta > v_0/v_1$. For dips less than this, a head wave will always be possible if the shot offset is large enough:

$$h > z_1\tan(\theta_c+\delta). \tag{3}$$

The minimum depth at which the head wave can be observed will be determined by

$$z \geq \frac{(2z_1+h\tan\delta)\tan\theta_c - h}{\tan\theta_c - \tan\delta}. \tag{4}$$

Note that the head wave will be visible at all phone depths from the surface to the interface at z_1 if the offset h is large enough. This is most likely to occur for a bed dipping upwards toward the shot. The amount of offset needed for the head wave to be recorded for all phones above the interface is

$$h \geq \frac{2z_1\tan\theta_c}{1-\tan\theta_c\tan\delta}.$$

The traveltime for a head wave from the shot to a phone at depth z is given by

$$t_h = \frac{1}{v_1}\left[\left[(2z_1-z)\cos\delta+h\sin\delta\right]\cot\theta_c+h\cos\delta-z\sin\delta\right]. \tag{5}$$

For a flat reflecting interface ($\delta=0$), the relations given above simplify considerably. Equation (2) for the reflection traveltime reduces to

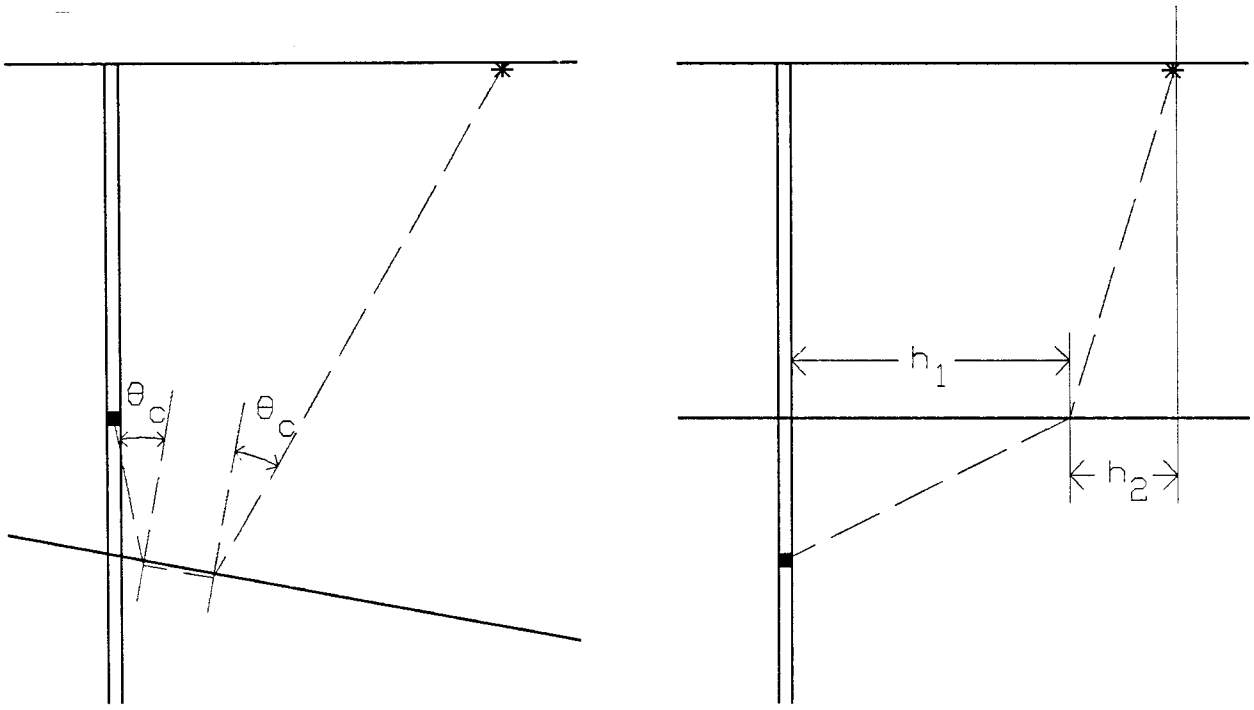

FIG. 3. (a) Ray path for a head wave (b) Ray path for transmitted or converted arrivals.

$$t_r = \frac{1}{v_0}\left[h^2+(2z_1-z)^2\right]^{1/2} \tag{2a}$$

The inequality in (3) determining existence of the head wave becomes

$$h > z_1 \tan\theta_c = \frac{z_1 v_0}{(v_1^2-v_0^2)^{1/2}} \tag{3a}$$

and the inequality in (4) giving the minimum depth for seeing the head wave becomes

$$z \geq 2z_1 - \frac{h(v_1^2-v_0^2)^{1/2}}{v_0}. \tag{4a}$$

The zero-dip head wave traveltime is specified by

$$t_h = \frac{h}{v_1} + \frac{(v_1^2-v_0^2)^{1/2}}{v_0 v_1}(2z_1-z). \tag{5a}$$

The head wave arrival produces an upgoing event, linear in h and z. The slope on a depth versus time profile will not be $\frac{1}{v_1}$ as might be expected from experience with normal reflection field profiles, but instead will be steeper (lower velocity) by a factor which is dip dependent:

$$\frac{1}{v_{effective}} = \frac{1}{v_1}(\cos\delta\cot\theta_c - \sin\delta) = \frac{1}{v_0}\cos(\theta_c + \delta).$$

In the flat interface case, this reduces to

$$\frac{1}{v_{effective}} = \frac{(v_1^2 - v_0^2)^{1/2}}{v_1 v_0}$$

Further calculation shows that, for the case of $z = z_1$,

$$t_d^2 - t_h^2 = \left[\left(\frac{(v_1^2 - v_0^2)^{1/2}}{v_1 v_0}(z\sin\delta - h\cos\delta)\right) + \frac{1}{v_1}(z\cos\delta + h\sin\delta)\right]^2.$$

The quantity on the right hand side is always non-negative, so for the geophone at the depth of the interface, the head wave never arrives later than the direct wave. This, then, provides an explanation of the upgoing 'hump' seen in figure 1; it is caused by the presence of a head wave in the data, with the head wave forming the first arrival for the geophones immediately above the interface.

Modeling of offset VSP arrivals

The equations derived above may be used to create simple traveltime models for offset VSP records such as Figure 1. For ease of comparison, the basic geometry of the experiment in Figure 1 was retained. The shot was offset 7000 feet from the well and phone depths ranged from 3300 to 13800 feet. The only interface introduced was a single horizontal reflector at a depth of 10700 feet. Equations 1, 2a and 5a were used to determine the direct, reflected and head wave arrival times.

Arrivals corresponding to a transmitted compressional (p) wave and a converted compressional to shear (p-s) wave were also calculated. The geometry of such an arrival is shown in Figure 3b. The travel time is given by

$$t_t = \frac{1}{v_0}(h_1^2 + z_1^2)^{1/2} + \frac{1}{v_1}\left[h_2^2 + (z - z_1)^2\right]^{1/2}$$

For application of this equation, Snell's law must be applied to eliminate h_1 and h_2 in favor of the known quantity h. This becomes cumbersome, so Fermat's principle was applied directly

and numerical rootfinding was used to solve

$$0 = \frac{dt}{dh_1} = \frac{h_1}{v_0}(h_1^2 + z_1^2)^{-1/2} - \frac{h_1}{v_1}\left[(h-h_1)^2 + (z-z_1)^2\right]^{-1/2}$$

for h_1, which then could be substituted into the travel time equation.

Extreme velocity contrasts were deliberately chosen for the first model to provide clear separation of the different events. The compressional wave velocity in the upper medium was taken to be 4500 feet/second. The lower medium compressional velocity was set at 24000 feet/second and the lower shear wave velocity at 8000 feet/second. The results of this model are shown in Figure 4. The different events are well separated and clearly identifiable. Because of the high velocity contrast used, a head wave is present everywhere above the depth of the reflecting horizon. The 'hump' caused by the head wave arriving sooner than the direct arrival below 10200 feet is pronounced. Because the upper compressional and lower shear velocities are similar, the p-s converted wave appears to continue the direct arrival through the interface.

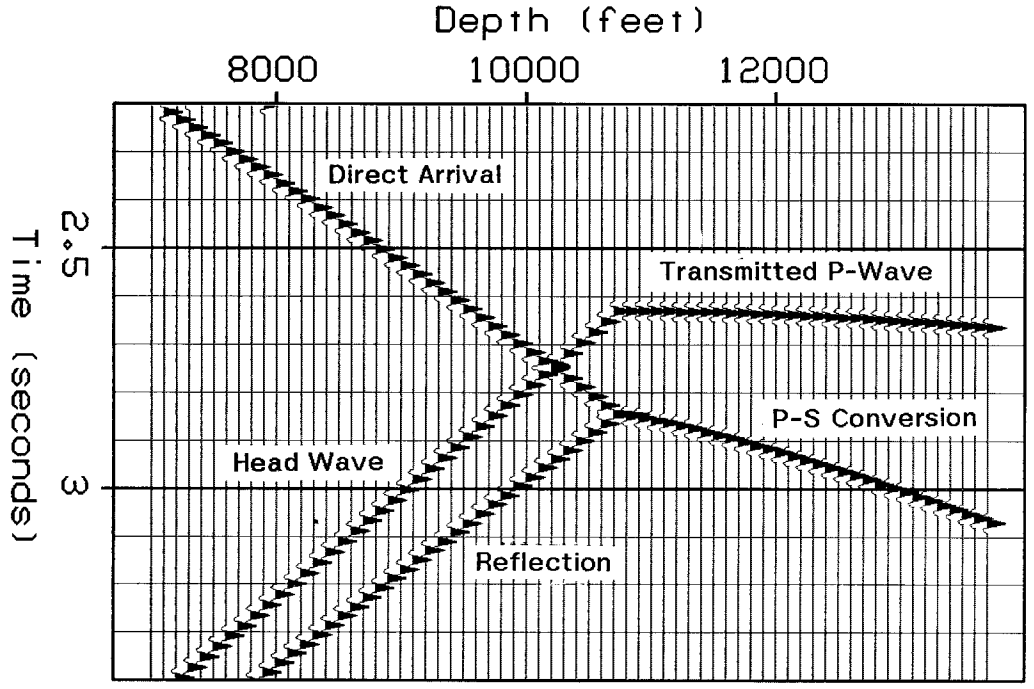

FIG. 4. Model 1: v_0=4500 ft/s, v_{1p}=24000 ft/s, v_{1s}=8000 ft/s

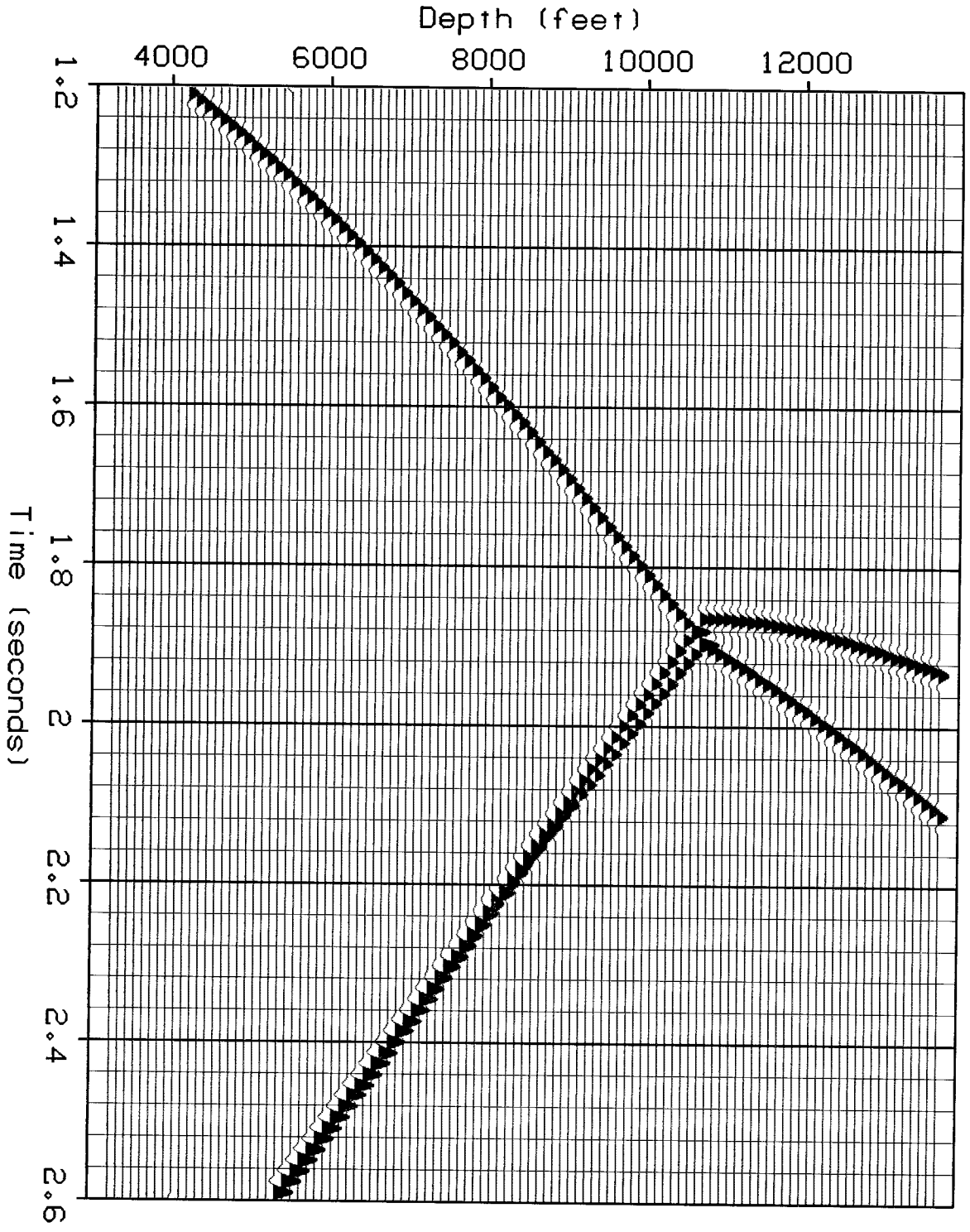

FIG. 5. Model 2: v_0=6750 ft/s, v_{1p}=17500 ft/s, v_{1s}=10000 ft/s

A more realistic attempt to fit the pattern of the data in Figure 1 produced Figure 5. The velocities used were estimated from Figure 1 and from the observer's notes which accompanied the data. Compressional velocities used were 6750 and 17500 feet/second in the upper and lower layers, respectively. Shear wave velocity in the lower medium was set arbitrarily at 10000 feet/second. Figure 5 matches well the general features of the traveltimes of events in Figure 1. The 'hump' in the first break curve appears as it is in the field data. The velocities chosen result in an apparent head wave velocity of 7316 feet/second, and a minimum depth of 4656 feet to see the head wave event. This can explain why the head wave is not seen as a second arrival distinct from the reflection above the depth at which the head wave and direct arrival curves cross; its apparent velocity is too similar to that of the reflection. Moreover, as Gal'perin (1974) points out, the head wave amplitude typically will be less than that of the reflection. Only traveltimes were modeled here and no attempt was made to calculate amplitudes or changes in waveform.

The most obvious discrepancy between the model of Figure 5 and the data of Figure 1 is the steeper direct arrival curve at shallow depths in the model. This is a consequence of using a single homogeneous upper layer with no velocity gradient. In most uses of offset VSP, detailed knowledge of the depths to interfaces and of velocity structure would be available from well logs, and would allow more sophisticated ray tracing methods to be used if needed. However, even the simple modeling presented here clearly shows that a large, but geologically realizable, velocity contrast is required to generate the head wave seen in the data of Figure 1.

In this paper I have tried to show how a head wave can be recognized in offset VSP data. Head waves are not restricted only to shallow depths, as the data discussed here show. When present, head waves may be difficult to distinguish from reflections and, by interfering with the waveform of the reflections, might complicate interpretation or processing of upgoing reflections. The magnitude of offset which could be used in VSP without generating head waves along a given interface can be estimated readily if the overlying rocks are relatively homogeneous.

ACKNOWLEDGMENTS

I thank Western Geophysical Company and Amoco Production Company, who provided the data set. I also thank Stew Levin for useful suggestions and discussion.

REFERENCES

Balch, A. H., Lee, M. W., Miller, J. J., and Ryder, R. T., 1982, The use of vertical seismic profiles in seismic investigation of the earth: Geophysics, v.47, p. 906-918.

Gal'perin, E. I., 1974, Vertical seismic profiling: Tulsa, SEG Spec. Pub. no. 12, p. 270.

Hardage, B. A., 1981, An examination of tube wave noise in vertical seismic profiling data: Geophysics, v.46, p. 892-903.

Lash, C. C., 1980, Shear waves, multiple reflections, and converted waves found by a deep vertical wave test (vertical seismic profiling): Geophysics, v.45, p. 1373-1411.

Lash, C. C., 1982, Investigation of multiple reflections and wave conversion by means of a vertical wave test (vertical seismic profiling) in southern Mississippi: Geophysics, v.47, p. 977-1000.

Ullmann, R., 1982, The separation of events on vertical seismic profiles, SEP-32, p.161-171.

Wyatt, K. D. and Wyatt, S. B., 1981, The determination of subsurface structural information using the vertical seismic profile: 51st Annual International SEG Meeting, Los Angeles, Ca.